Structure of the Reduced TiO_2(110) Surface Determined by Scanning Tunneling Microscopy

Gregory S. Rohrer,* Victor E. Henrich, Dawn A. Bonnell

The scanning tunneling microscope has been used to image a reduced TiO_2(110) surface in ultrahigh vacuum. Structural units with periodicities ranging from 21 to 3.4 angstroms have been clearly imaged, demonstrating that atomic resolution imaging of an ionic, wide band gap (3.2 electron volts) semiconductor is possible. The observed surface structures can be explained by a model involving ordered arrangements of two dimensional defects known as crystallographic shear planes and indicate that the topography of nonstoichiometric oxide surfaces can be rather complex.

[version 9/17/90]

G. S. Rohrer, Department of Metallurgical Engineering and Materials Science, Carnegie Mellon University, Pittsburgh, PA 15213.
V. E. Henrich, Surface Science Laboratory, Department of Applied Physics, Yale University, New Haven, CT 06520.
D. A. Bonnell, Dept. of Materials Science and Engineering, University of Pennsylvania, Philadelphia, PA 19104.

Transition metal oxide surfaces play an important role in a number of interesting phenomena including heterogeneous catalysis, gas sensing, electrode/electrolyte interactions, and bonding at metal/ceramic interfaces. However, in comparison to the current knowledge of metallic and covalently bonded semiconductor surfaces, little is known about transition metal oxide surfaces. Notable successes among the few scanning tunneling microscope (STM) studies of oxides include the atomic or near-atomic resolution imaging of four different metallic oxide surfaces (1) and the imaging of some atomic-scale features on the surface of $Rb_{0.05}WO_3$, a semiconducting tungsten bronze (2).

We have used the STM to study the geometric and electronic structure of the TiO_2(110) surface, a wide band gap, semiconducting oxide. We acquired images from a single crystal TiO_2(110) sample that was cleaned and annealed in ultrahigh vacuum (UHV), conditions necessary to avoid the adsorption, band bending, and charging effects which are known to occur in air. Several well-ordered areas have been imaged that contain a variety of atomic-scale, periodic structures. Although none of these features correlate with the expected surface structure, they are consistent with a model involving the presence of crystallographic shear (CS) planes that accommodate local variations in stoichiometry. We briefly describe two of the observed structures and compare them to the proposed model.

Titania can support a wide range of oxygen deficiency (TiO_{2-x}, x = 0 to 0.33) through the formation of planar defects known as CS planes which, when numerous enough, order to form new compounds with distinct compositions and structures that are known as Magneli phases

(3). The general formula for these compounds, which can occur as intergrowths in reduced crystals, is Ti_nO_{2n-1} where $n \geq 3$. The n^{th}-order CS structure may be formed by creating oxygen vacancies at the anion sites in every $2n^{th}$ shear plane (for example, the (121) plane) and displacing the adjacent rutile section by $^1/_2$[011]. The result is that the approximately close-packed O framework remains continuous but the Ti cations are in antiphase locations, with increased Ti concentration along the shear planes (Fig. 1).

Several groups have previously produced STM images of single crystal titania surfaces (4). None of these studies, however, produced atomic resolution images, four having been carried out in air and the fifth in an electrolyte solution. Our TiO_2(110) single crystal was cleaned, annealed, and characterized in UHV (5). Low-energy electron diffraction (LEED) patterns indicated the presence of a well-ordered, relatively defect-free surface (6). The crystal was then exposed to air for several days before being introduced into the UHV STM chamber, where it was heated at approximately 673 K for 2 min and then 'flashed' at approximately 973 K for 5 s. A (1X1) LEED pattern was found after this treatment that was identical to that observed following the initial preparation. Orientation of the crystal during STM analysis was determined from the LEED pattern. The orientation of the images are within ± 10° of the crystal orientation, the primary source of error being thermal drift.

We imaged the sample using a commercial STM head (7) controlled by "homemade" feedback electronics and software of conventional design. The mechanically formed Pt tip was "sharpened" *in situ* by applying a 90 V potential between the sample and tip and

passing 1 μA of current for several minutes. The procedure had to be repeated periodically to maintain tip resolution and stability. The dependence of the tunneling current on sample-tip separation was used to gauge the integrity of the vacuum gap. The standard vacuum tunneling equation was used to compute values of the effective barrier height between 4.2 and 5.0 eV (8). All of the images we present here were collected in the constant current mode at a 2.0 V sample bias with respect to the tip and a 0.1- nA tunneling current and are presented after the subtraction of a background plane, which eliminates the tilt of the sample that would otherwise overwhelm small variations and make atomic features undetectable.

Well-ordered areas were visible on the majority of the surface (> 50 % when the tip was sharp), but observed less frequently after several days of analysis. Two of the observed structures are discussed below. Auger electron spectroscopy (AES) performed immediately after the initial thermal treatment and at the end of the STM analysis showed that the level of carbon contamination had increased, presumably through exposure to background gases in the vacuum chamber. Fourier analysis and direct measurement of the images in Fig. 2A and B indicates that the rows oriented in the [111] direction have an 8.5 Å periodicity and a 1 Å corrugation height. The corrugation directed along the rows has a 3.4 Å periodicity and a 0.2 Å amplitude. The width of these rows seems to vary somewhat and there are also numerous "missing cells." The bulk-terminated rutile lattice vectors have been added for comparison.

The image in Fig. 2B shows a larger area containing two ledges or atomic steps that are 2.2 Å in height, which is significantly less than the

distance between adjacent (110) planes, which is 3.25 Å. Some regions of the image are either disordered or covered with adsorbates. Notice that the dark line that cuts across the image in Fig. 2B in the [113] direction (indicated by the arrow on the top left side of the image) and that forms a step edge in the lower portion of the picture. This feature is the same direction in which the rows and ledges found in Fig. 3, acquired from a different area of the crystal surface, are oriented. The largest rows in Fig. 3B, oriented in the [113] direction, are approximately 20 Å wide and are parallel to the large steps visible in Fig 3A. The height of the step in Fig. 3B is 9 Å. The detail in Fig 3C shows that each row is composed of discrete units arranged in a roughly hexagonal pattern. The structure shown in Fig. 2 differs from the one shown in Fig. 3, and neither can be explained by a simple surface termination of the bulk unit cell or some combination of unit cells.

Two possible models can account for the observed surface structures, both of which rely on the presence of bulk nonstoichiometry. The geometries of both of the experimentally observed surface structures can be simply created by removing oxygen from the surface layer in the appropriate pattern; we call this the ordered-surface oxygen vacancy (OSOV) model. However, an STM image is not simply a reproduction of the surface geometry, but also depends on the surface density of states. Because all of the images were acquired at positive sample bias, electrons tunneled into unoccupied conduction band states that are predominantly Ti in origin. It follows that the light spots on the image reflect a greater density of Ti states, associated with the Ti atom positions, whereas the dark areas between the rows correspond to the absence of Ti states that occur at the O atom positions. This result

suggests that O must reside at the dark positions along the [111] and [113] directions while the other sites are vacant. However, at these positions, the tip is displaced downward by 1 Å, a rather large corrugation to arise from a change in the local density of states alone, especially considering that the presence of O atoms in these positions would presumably cause an additional opposite corrugation from purely geometric considerations. Because of this contradiction, the OSOV model does not seem plausible.

The second model, the crystallographic shear (CS) model, avoids this contradiction by assuming that the major row corrugations are actually steps that would result naturally from CS displacements. The CS displacements can occur along a variety of planes including the (121) family of planes. The (121) plane intersects the (110) surface along the [111] direction, the same direction that the rows in Fig. 2 are oriented. The intersection of the (121) plane the (110) surface is in the direction [113], the same direction in which the rows in Fig. 3 are aligned. The CS displacement is always of the type $^1/_2$[011], which means that adjacent sections of the crystal are vertically displaced 1.6 Å with respect to one another along the line normal to the (110) surface. Because the plane subtraction applied to each image removes any global slope, a stepped structure appears saw-toothed, so that the intersection of each CS plane with the surface appears as a depression or dark spot on the image.

The presence of excess Ti along the crystallographic shear planes should result in a corrugation which is opposite to the geometric effect. However, corrugations due to alterations in the electronic density of states are usually some tenths of angstroms, so this effect should not be able to cancel the larger geometric effect. In fact, the observation that

the corrugations in Fig. 2 are about 1 Å, less than the expected value of 1.6 Å, suggests that the presence of excess Titanium in these positions compensates somewhat for the geometric effect. The disagreement between the expected and measured step height mentioned earlier may also be explained if each step is actually the sum of one (110) interplanar spacing and a CS plane. Although previous models of the reduced TiO_2(110) surface have not considered the possible existence of CS planes or their effect on the titania surface structure (9), the existence of these planar defects has been proposed by Firment et al. (10) to explain angle-resolved UPS data from the reduced MoO_3(010) surface, another transition metal oxide that forms a variety of CS structures.

The spacing of the rows in Fig. 2 suggests that every sixth anion (121) plane is a CS plane and that the local composition in this area is Ti_3O_5, while the spacing of the rows in Fig. 3 suggests that CS occurs at every twelfth anion (121) plane and that the local composition is Ti_6O_{11}. Although these phases are known to have a higher conductivity than rutile, they are still semiconducting, a fact verified by tunneling spectroscopy measurements. The 0.2 Å corrugations within the rows of Fig. 2 have a 3.4 Å spacing which is very close to the spacing of Ti atoms (3.5 Å) along this same direction in the ideal rutile unit cell. Apparently the nearest neighbor Ti atoms, separated by only 3 Å along the c axis, are not resolved. The distance between adjacent units within the rows of Fig. 3, measured parallel to the [110] direction, is approximately 6.4 Å, close to the bulk rutile unit cell spacing in that direction (6.5 Å). The distance between adjacent units in the [113] direction is 5.6 Å, which is the distance between the neighboring Ti atoms in that direction.

However, each Ti atom is clearly not imaged and a more detailed model for the atomic structure within the rows will have to be formed on the basis of additional experiments.

References and Notes

1. M. D. Kirk et al., Science **242**, 1673 (1988); N. J. Zheng, U. Knipping, I. S. T. Tsong, W. T. Petuskey, J. C. Barry, J. Vac. Sci. Technol. **A 6**, 457 (1988); E. Garfunkel et al., Science **246**, 99 (1989); X. L. Wu, Z. Zhang, Y. L. Wang, C. M. Lieber, ibid. **248**,1211 (1990).

2. M. L. Norton, J. G. Mantovani, R. J. Warmack, J. Vac. Sci. Tech. A **7**, 2898 (1989).

3. L. A. Bursill and B. G. Hyde, Prog. Solid State Chem. **7**, 177 (1972).

4. S. E. Gilbert and J. E. Kennedy, J. Electrochem. Soc. **135**, 2385 (1988); K. Itaya and E. Tomita, Chem. Lett., 285 (1985); K. Sakamaki, S. Matsunaga, K. Itoh, A. Fujishima, Y. Gohshi, Surf. Sci. **219**, L531 (1989); S. E. GIlbert and J. H. Kennedy, Langmuir **5**, 1412 (1989); Surf. Sci. **225**, L1 (1990).

5. The 1.0 mm 5 mm 1.6 mm titania sample was oriented to within ± 1/2° of the (110) face by Laue diffraction and cut with a high-speed diamond saw from a single-crystal boule. The surface was polished by sequentially reducing the size of Al_2O_3 grinding media down to 1 µ. The crystal was then reduced in UHV by annealing in a resistively heated tantalum boat at a temperature above 900 K (based upon color) for 36 hours. Following this treatment, the crystal was dark gray in color and opaque. The surface was then argon-ion milled for 5 min at 2 kV followed by 25 min of ion

bombardment at 500 V using an estimated current density of 5 to 10 μA/cm^2. The crystal was then annealed at 823 K for 30 min in 1 X 10^{-7} torr of oxygen in order to re-oxidize the surface and anneal out the damage produced by ion bombardment.

6. No ultraviolet photoelectron spectroscopy (UPS) data were taken on this surface, although the LEED patterns were similar to those on the TiO_2(110) surfaces that exhibit no band gap defect surface states; see H. R. Sadeghi and V. E. Henrich, Appl. Surf. Sci. **19**, 330 (1984).

7. The STM head was manufactured by WA technologies, Cambridge, England.

8. For details on the determination of the apparent barrier height, see J. K. Gimzewski and R. Moller, Phys. Rev. **B 36**, 1284 (1987); N. D. Lang, ibid, p. 8173; and G. Rohrer and D. Bonnell, J. Am. Ceram. Soc., in press.

9. W. Gopel, G. Rocker, R. Feierabend, Phys. Rev. **B 28**, 3427 (1983); V. Henrich, Rep. Prog. Phys. **48**, 1481 (1985).

10 L. E. Firment, A. Ferretti, M. R. Cohen, R. P. Merrill, Langmuir **1**, 166 (1985).

11. Supported at the University of Pennsylvania by IBM Research and the National Science Foundation and at Yale University by the National

Science Foundation solid state chemistry division grant DMR-8711423. We thank Z. Zhang for assistance in preparing the sample surface.

Fig. 1. Illustration of the CS plane formation process and the effect on the topography of the (110) surface. For simplicity, the structure is viewed parallel to the (100) direction in (A to C), while (D) is a perspective drawing that illustrates the effect of this operation on the (110) surface. (A) Idealized rutile structure; the larger circles represent O and small black circles represent Ti. (B) Oxygen vacancies formed along the (121) plane. (C) Translation of one-half of the structure [the parts to the right of the (121) plane shown in (B)] by the vector 1/2[011] reestablishes the close-packed O framework and leaves the Ti atoms in antiphase positions. (D) The shear operations produce an ordered arrangement of steps on the (110) surface, as depicted in this perspective drawing. In this case, the steps are oriented in the [111] direction.

Fig. 2. (A) An STM image showing a 109 Å by 109 Å area of the TiO_2(110) surface. The vertical resolution from black to white is 2 Å, with lighter shades corresponding to topographic peaks. (B) A 246 Å by 246 Å area that includes several steps. The vertical resolution from black to white is 2.8 Å. (C) Profile taken along the line indicated in (B) shows the height of the steps.

Fig. 3. (A) An STM image of a large terraced area (930 Å by 379 Å) with a series of steps oriented in the [113] direction. The vertical

resolution from black to white is 43 Å. (B) A more detailed scan (273 Å by 108 Å) of a region on the right side of (A). The vertical resolution from black to white is 9 Å. (C) An enlargement of a subsection of this image shows detail within each row.

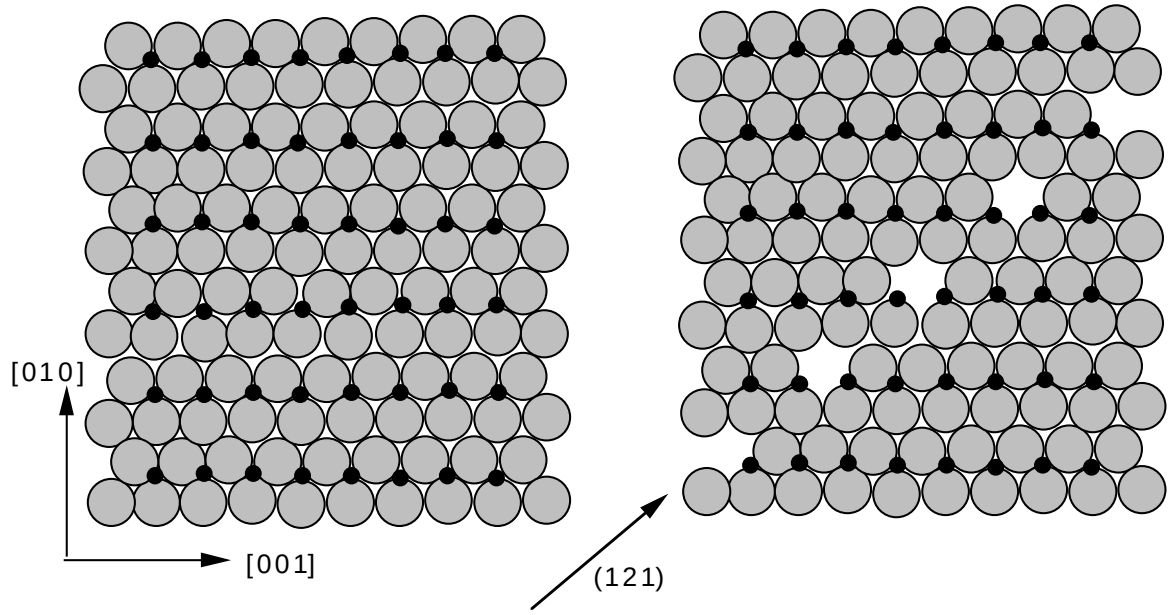

a) b)

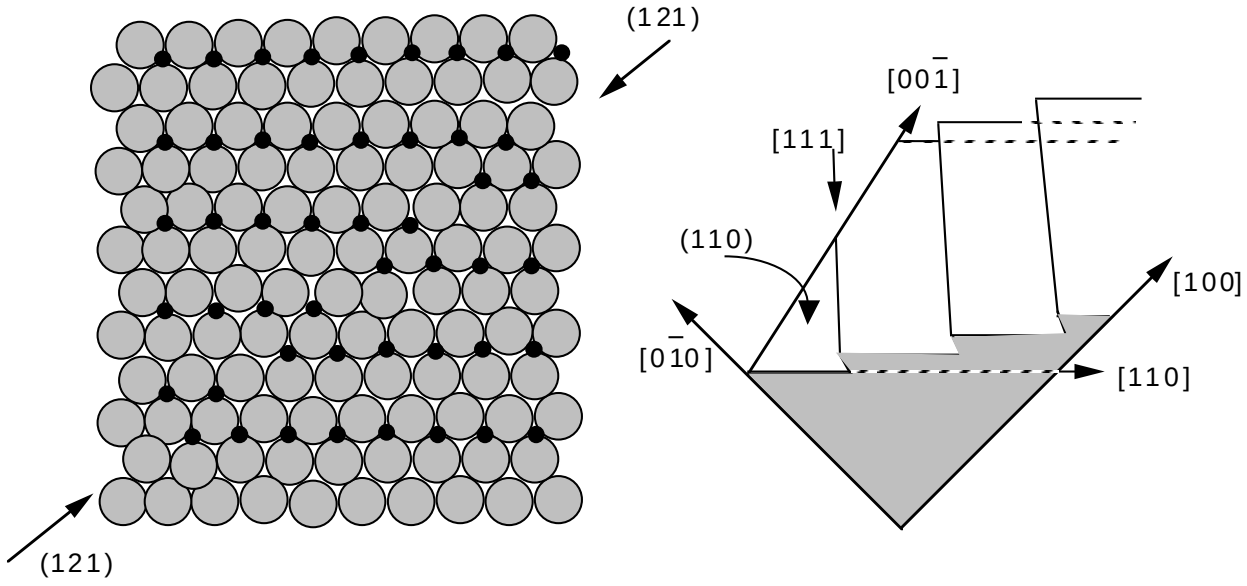

c) d)

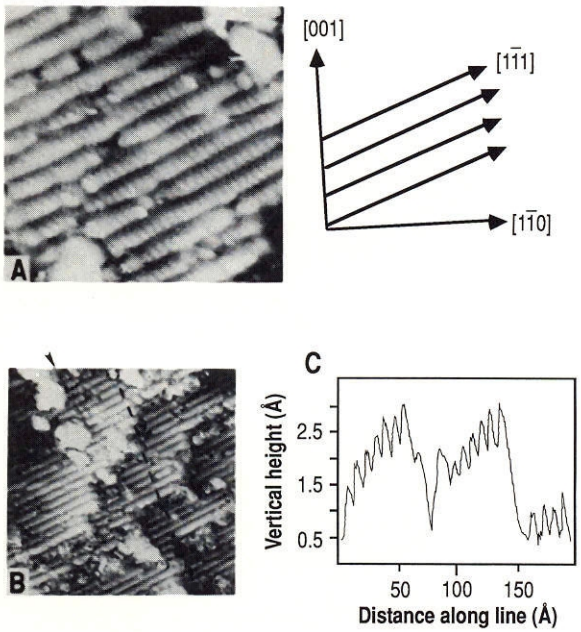
A
[001]
[1$\bar{1}$1]
[1$\bar{1}$0]
B
C
Vertical height (Å)
2.5
1.5
0.5
50
100
150
Distance along line (Å)

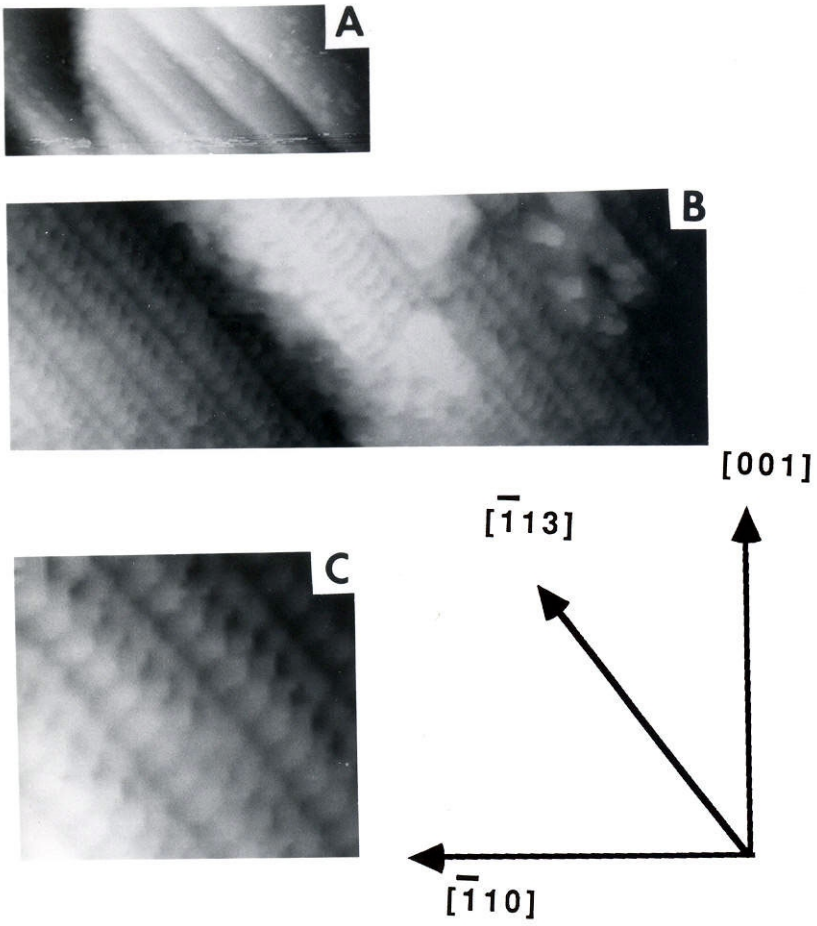
A
B
C
[001]
[$\bar{1}$13]
[$\bar{1}$10]